Dynamic Simulation of Seismic Excitation on Dipping Faults: the Importance of Dynamic Source Effects on Strong Ground Motion Prediction

Dalguer, Luis Angel[1,2)], Riera, Jorge Daniel[2)] and Irikura, Kojiro[1)]

1) Disaster Prevention Research Institute, Kyoto University, Uji Kyoto 611-0011, Japan
2) Federal University of Rio Grande do Sul, Porto Alegre, Brazil

ABSTRACT

Earthquakes on dipping faults generate large differences between the near-source ground motion at the hanging wall and at the footwall, the ground motion in the hanging wall being larger than in the footwall. This effect was distinctly observed in the recent 1999 Chi-Chi (Taiwan) earthquake (Ms= 7.6) in which the rupture of the causative fault of the earthquake reached the surface and propagated along 80 km. Unusually large vertical displacements, between 1.0 and 4.0m, as well as horizontal displacements of up to 8.0m, were registered along the fault trace on the hanging wall. No earthquake with such characteristics had previously been recorded, so the event had an immediate impact in the fields of seismology and earthquake engineering. In order to show that the ground motion on dipping faults that break the free surface is affected mainly by dynamic source effects, the rupture process of dipping faults with different asperity size but with the same seismic moment is modeled. The results suggest that the effect of the asperity size on ground motion is important in the generation of high frequency components. The smaller the asperity, the larger are the high frequency components generated. Based on these results, we simulate the rupture process of the southern and northern parts of the 1999 Chi-Chi (Taiwan) earthquake in order to explain the damage distribution on buildings caused by the earthquake in which, although the strongest ground motion occurred at the northern part of the causative fault, structural damage was heavier in the southern part. In addition, the rupture process of the thrust fault near the hypocenter area of the 1999 Chi-Chi (Taiwan) earthquake was compared with another similar model in which the rupture is forced to stop 3 km before it reaches the surface. From the results, it can be clearly seen that the effect of the rupture reaching the surface cannot be disregarded in predictions of the ground motion in the vicinity of the surface trace. A 2D Discrete Element Model (DEM) was employed to perform a dynamic simulation of the rupture process of the fault and the near-fault ground motions. The resulting equations of the elastodynamic problem were solved for a region around the causative fault, using explicit time integration. The dynamic model presented herein shows the importance of an adequate consideration of the source process in ground motion prediction and the potential of the approach to complement seismic risk studies.

INTRODUCTION

Earthquakes on dipping faults generate asymmetrical distributions of near-source ground motions because of the asymmetric geometry of the hanging and the footwalls. The motion on the hanging wall is larger than on the footwall. Analyses of strong ground motion data from recent reverse and normal earthquakes show these characteristics. The 1994 Northridge [1], the 1971 San Fernando and the recent 1999 Chi-Chi (Taiwan) earthquakes produced higher levels of ground motion on the hanging wall sides than on the footwall sides The investigation of the rupture process of the 1961 Kita-Mino earthquake in central Japan [2], and reports of theoretical dynamic simulations of dipping faults (See for example[3] and [4]) as well as the foam rubber experiments of Brune [5], have also suggested larger motions occur on the hanging wall.

In the recent investigation of the dynamic rupture process of the southern part and northern part of the causative dipping fault of the of the 1999 Chi-Chi (Taiwan) earthquake (see [6] and [7]), it was also observed that the faulting generated large differences between the near-source ground motions at the hanging wall and at the footwall. The ground motion in the hanging wall is larger than in the footwall, these numerical simulations suggesting that such a difference is principally caused by the asymmetric geometry of the hanging and footwalls. For this earthquake, where the rupture of the fault reaches the surface, the effect of the asymmetry on the ground motion is considerable.

The understanding of the dynamic source process of dipping faults that break the surface is still relatively limited. This was due to the difficulty of access to the seismogenic zone and to the lack of strong motion data near the source. However, a seismic instrumentation program was successfully implemented in Taiwan three years ago by the Central Weather Bureau (CWB), just in time before the disastrous 1999 Chi-Chi earthquake, providing a wealth of modern digital records for seismology and earthquake engineering. Certainly, these data will encourage earthquake research leading to an improved understanding of this type of earthquake.

In order to show that the ground motion on dipping fault that break the free surface is influenced mainly by dynamic source effects, the rupture process of dipping faults with different asperity sizes but with the same seismic moment is

modeled. The results suggest that the effect of the asperity size on ground motion is important in the generation of high frequency components. The smaller the asperity, the larger are the high frequency components generated. Based on these results, we simulate the rupture process of the southern and northern parts of the 1999 Chi-Chi (Taiwan) earthquake, in order to explain the distribution of damage on buildings caused by the earthquake. In addition, the rupture process of the thrust fault near the hypocentral area of the 1999 Chi-Chi earthquake (southern part) was compared with a similar model in which the rupture is forced to stop 3 km before it reaches the surface. The results of the simulations are discussed in this paper.

THE 1999 CHI-CHI (TAIWAN) EARTHQUAKE

The recent 1999 Chi-Chi (Taiwan) earthquake (Ms= 7.6) had a serious impact in the international community of scientists and engineers devoted to seismology and earthquake engineering because of its complexity and uncommon characteristics. The earthquake originated on a low-angle reverse fault with a strike of nearly N5° E and a dip between 25° and 36° [8]. The rupture of the causative fault reached the surface and propagated along about 80km, starting at the southern and extending northwards of the Chelongpu fault, as shown in Fig. 1a. Spectacular horizontal displacements up to 8.0 m and vertical offsets of 1.0m to 4.0m were registered along the surface rupture, being the largest on the northern zone. The damage caused by the earthquake shows an uncommon distribution. Although the largest displacements occurred at the northern part of the causative fault, structural damage was heavier in the southern part. Heavy damage happened mostly in the hanging wall side and less in the footwall side. Such differences in the damage distribution can be inferred from Fig. 1b, which presents a comparison of the spectral pseudo-velocity from records of stations located at the northern (TCU052) and southern (TCU129 and TCU089) parts. The peak velocity for frequencies less than 1.0 Hz is larger in the northern part. On the contrary, for frequencies greater than 1.0 Hz, the peak velocity ground motion is larger in the southern part. It means that the northern part generated stronger ground motion in low frequency than the southern part. As previously indicated, in order to gain a better understanding of the complex damage distribution caused by this earthquake, the rupture process was numerically simulated. First, we simulated the rupture process of three theoretical dipping faults with different asperity sizes, but with the same seismic moment. These simulations were made in order to study the effects of the asperity on the ground motion. The results show that the model with the smallest asperity generated stronger ground motions in the high frequency range.

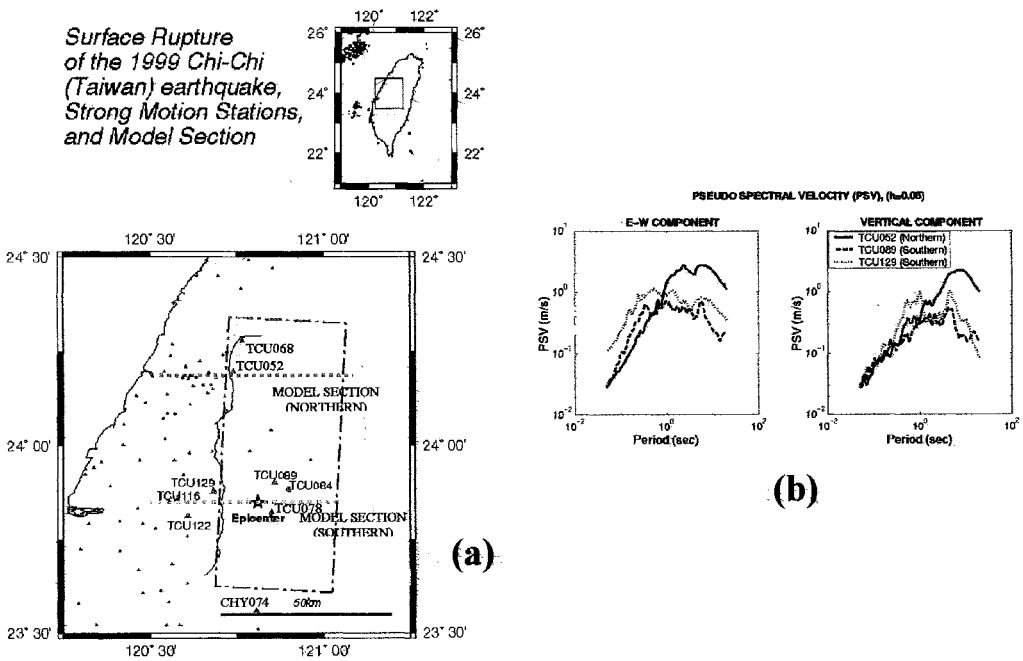

Fig. 1. a) Location of the surface rupture of the Chelongpu fault, stations records used for comparison, source model and sections of the northern and southern model; b) Comparison of pseudo spectral velocity for records of stations at the northern and southern parts.

DESCRIPTION OF THE NUMERICAL SOLUTION

The Discrete Element formulation (DEM), used in the analysis, models any orthotropic elastic solid by means of a three dimensional periodic lattice structure in a cubic array. Nayfeh and Hefzi [9] determined the equivalent stiffness of the elements in the cubic arrangement, in order to model an orthotropic elastic medium. It has been verified that the method leads to results that exactly converge to solutions for a linear isotropic elastic continuum, in static problems, for Poisson's ratio equal to 0.25. Negligible differences are observed for Poisso's ratio in the range 0.15 to 0.35. Riera and Rocha, [10] used the approach in dynamic fracture studies, Doz and Riera, [11] employed it to model the stick-and-slip motion in sliding bodies and Dalguer et al.[12] evaluated the generation of foreshock and periodicity of earthquakes. In the discrete dynamic model, masses are concentrated at nodal points. Solids are represented as an array of normal and diagonal elements linking lumped nodal masses. The dynamic analysis is performed using explicit numerical integration in the time domain. At each step of integration, a nodal equilibrium equation (Eq. 1) is solved by the central finite differences scheme.

$$m\ddot{u}_i + c\dot{u}_i = f_i \tag{1}$$

where m denotes the nodal mass, c the damping constant, u_i a component of the nodal coordinates vector and J_i a component of the resulting forces at the nodal point including elastic, external and frictional forces in direction i of the motion. In the current model, only the nodal points that coincide with the pre-existing fault are subjected to frictional forces, governed by the slip-weakening friction law. The damping constant c was assumed to be proportional to the stiffness (k) of the elements, that is $c=\xi k$, where ξ was assumed to be 0.005.

SIMULATION OF DIPPING FAULTS WITH DIFFERENT ASPERITY SIZES

Fig. 2a shows the fault model used to simulate the rupture process of a dipping fault. A simulation is performed for different asperity sizes but with the same seismic moment, as indicated below:

Model 1: Length of asperity L =6km, Stress drop on the asperity $\Delta\sigma$=9.0Mpa.
Model 2: Length of asperity L =8km, Stress drop on the asperity $\Delta\sigma$=5.0Mpa.
Model 3: Length of asperity L =10km, Stress drop on the asperity $\Delta\sigma$=3.2Mpa

All the models share the following common assumptions: (a) There is a surface sedimentary layer with a depth of 4km characterized by a set of P wave velocity (4.3 km/sec), S wave velocity (2.5 Km/sec), density 2500 kg/m^3. The basement (seismogenic zone) is a homogeneous medium with P wave velocity (6.1 km/sec), S wave velocity (3.5 Km/sec), density 2700 kg/m^3, (b) The slip-weakening friction model is adopted as the constitutive relation for the fault, (c) The stress drop along the fault plane in the shallow surface layer is negligible, (d) The ultimate stress, i.e. the strength excess on the fault surface in the shallow surface layer increases linearly with depth and, in order to avoid any fault opening, a normal stress along the fault, equivalent to the strength excess, is applied on the fault surface and (e) The critical slip (D_c) along the fault is larger near the surface than at greater depths.

The main results of these simulations are shown in Fig. 2b. The final displacements along the free surface are almost the same for the three models, because all the models have the same seismic moment. But if we observe the peak velocity along the fault, the model with asperity length L=6km shows higher values than the others. This difference increases when the ground motion is filtered in the frequency range from 0.5Hz to 2.0Hz. These results suggest that higher frequency motion is generated by the model with smallest size of asperity.

DYNAMIC RUPTURE PROCESS SIMULATION OF THE 1999 CHI-CHI (TAIWAN) EARTHQUAKE

Since the faulting process appears to have been nearly pure thrust along the various fault segments, a 2D model was employed to perform a dynamic simulation of the rupture process of the fault and the near-fault ground motion. On account of the differences in the observed features of the rupture process in the northern and southern parts of the causative fault of the 1999 Chi-Chi (Taiwan) earthquake, each part was modeled independently. The location of the two model sections along the surface rupture is shown in Fig. 1a. The first model (southern part) is near the epicentral area and the second model (northern part) is near the TCU052 station. The parameters used for the dynamic simulation and the geometry of the two fault models are shown in Fig. 3. Both models share the same common assumptions used for the three theoretical models presented in the previous section. In the model for the southern part, the existence of only one asperities with small width (6 km) and stress drop of 3Mpa were admitted in the basement underlying the sediments. The northern part, on the other hand, is assumed to have an asperity with larger width (15km) and higher stress-drop (between 1.5 MPa and 8MPa).The main

results of the simulation are described next. A comparison of the ground motion on the surface between the northern and southern models (in a frequency range up to 2.00 Hz) is shown in Fig. 4. This Figure shows the final displacements, peak velocity and peak velocity in a frequency range of 0.5 to 2.0Hz. In Figs. 4a and 4b it is observed that the final displacement and the peak velocity are larger in the northern model than in the southern model. However, when the ground motion

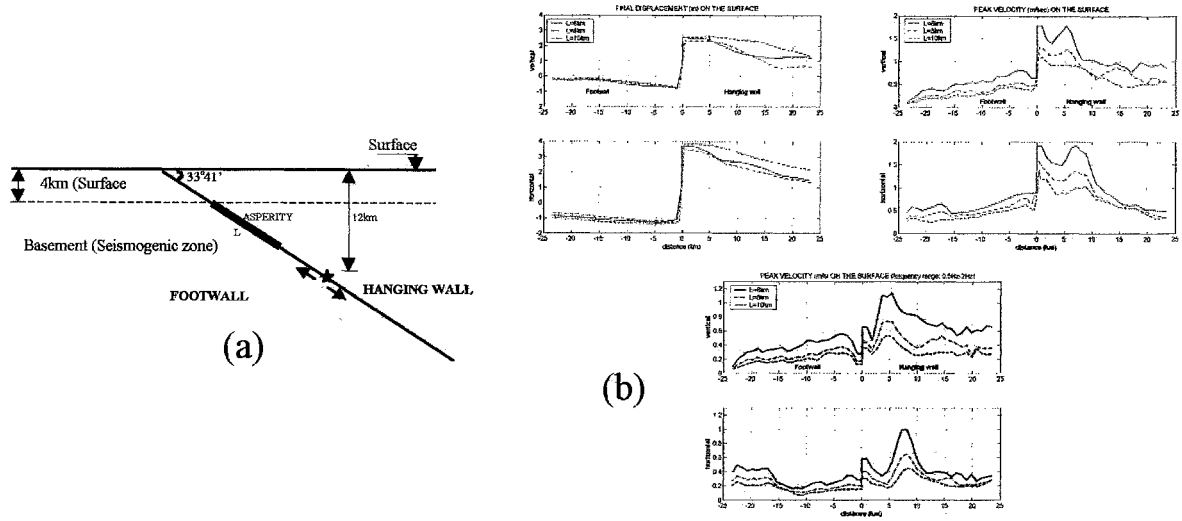

Fig. 2. a) Fault model used for the dynamic simulation of dipping faults with different asperity size (L=6km, L=8km and L=10km); b) Comparison of the final displacement and peak velocity on the surface between the three models with different size asperity.

velocities are filtered in a frequency range of 0.5 to 2.0Hz, as shown in Fig. 4c, the peak velocities are larger in the southern model than in the northern model. These results suggest that the northern model predicts stronger ground motion than the southern model in lower frequencies. However, in the higher frequency range between 0.5 to 2.0 Hz (natural frequency range of standard structures), the ground motion is stronger in the southern model. From these results we can conclude that although the northern model indicates stronger ground motion, the most severe damage in structures should take place in the southern part, because it was more prone to excite severely the fundamental frequency of standard structures.

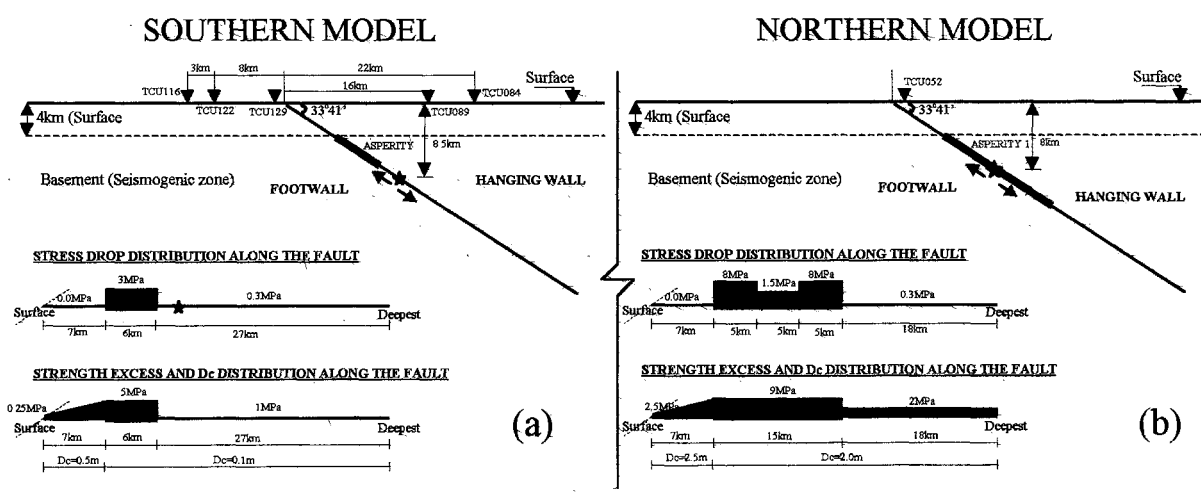

Fig. 3. Fault models and parameters distribution used for the dynamic simulation: (a) southern model, (b) northern model.

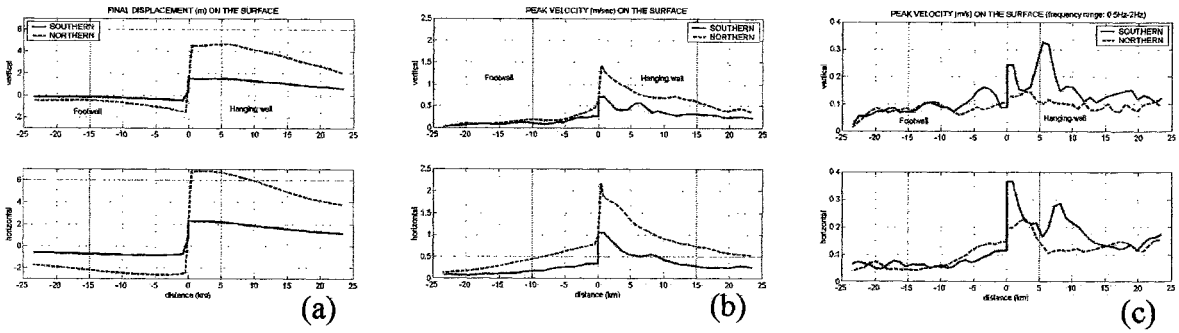

Fig. 4. Comparison of the final displacement and peak velocity on the surface between the northern model and southern model: (a) Final displacement, (b) peak velocity (c) peak velocity in a frequency range of 0.5 to 2.0 Hz.

In order to validate the dynamic models studied here, we next compare the results described above with actual observations. Figure 5 shows that the southern model predicts final vertical displacement of about 2.0m and horizontal displacement of about 3.3m in the hanging wall that agree satisfactorily with those obtained by the GPS data and the final displacements of the station records. In Figure 6a to 6e we also compare the waveform of the displacement and velocity ground motions of east-west and vertical components recorded at five stations near the surface rupture of the epicentral area (stations TCU084, TCU089 on the hanging wall side and TCU129, TCU116 and TCU122 on the footwall side). We find that the main characteristics of the recorded ground motions are adequately reproduced, by comparing simulated and observed time-histories. In the frequency range from 0.5Hz to 1.0Hz, although obtained with a 2D model, the ground motion simulation qualitatively matches the observations. And also for the northern model we succeed in simulating the ground motion recorded of TCU052 station, as shown in Figure 6f, in which simulation results fit quite well with recorded values. The dynamic models presented in this paper showed that the effects of the dynamic source mechanism on strong ground motion have fundamental importance in ground motion prediction in the epicentral area and in the assessment of seismic hazard

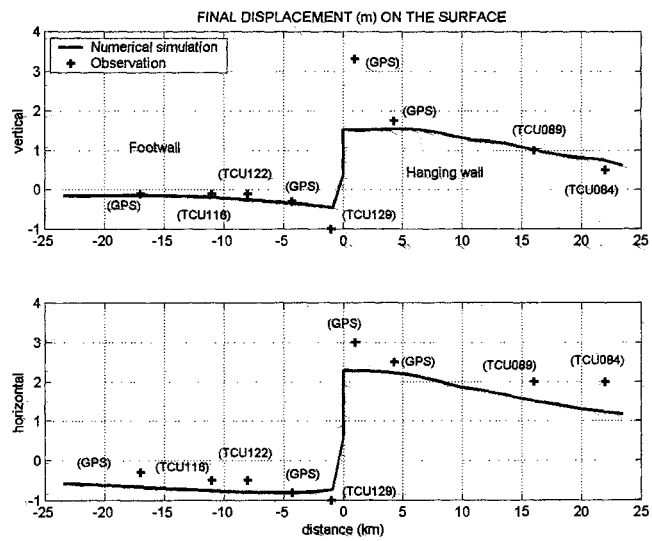

Fig. 5. Comparison between the numerical simulation and the observations (GPS data and stations records) of the final displacements along the surface near the epicentral area (southern model).

Finally, in order to observe the effects of the faulting when the rupture breaks the surface, in Fig. 6 we compare the final displacements and the peak velocities on the surface resulting from two dynamic source models:. The first is the southern model of the Chi-Chi earthquake shown in Fig. 3a, in which the rupture reaches the ground surface (solid line), while the second is a similar model in which the rupture is forced to stop 3 km before reach the surface (dashed line). It can be observed that the effect of the rupture reaching the surface on the ground motion very close to the surface trace is clearly noticeable. The final displacement as well as the peak velocity ground motion increase when the rupture breaks the ground surface.

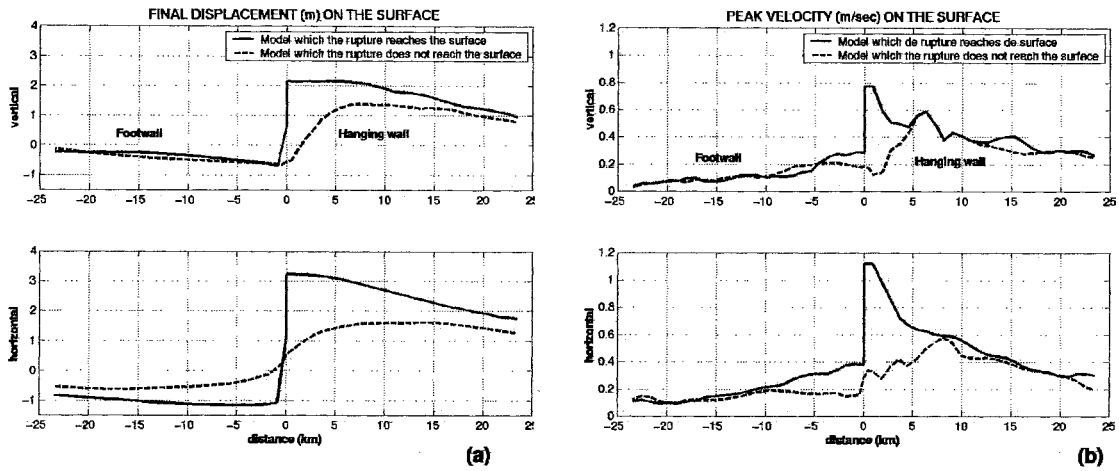

Fig. 6. Comparison between the southern model used to simulate the 1999 Chi-Chi earthquake that the rupture breaks the surface (solid line) and another model that the rupture does not reach the surface (dashed line): (a) vertical and horizontal component of the final displacement along the surface and (b) vertical and horizontal component of peak velocity along the surface

CONCLUSIONS

Using the simplified 2D discrete element method it was possible to show various aspects of the dynamic source effect on the strong ground motion of the 1999 Chi-Chi (Taiwan) earthquake. The ground motion simulation (southern part) shows satisfactory agreement with the observed records. This comparison with actual observations validates the results presented in this paper, which indicate that the ground motion near the fault of the 1999 Chi-Chi (Taiwan) earthquake was affected mainly by dynamic source effects. The simulations show that higher frequency motion is generated by the model with smallest asperity size. Therefore, due to these source effects, in the low frequency range the northern model (with large asperity) predicts stronger ground motion than the southern model (with small asperity). On the contrary, in the high frequency range, between 0.5 to 2.0 Hz, stronger ground motion was predicted by the southern model. It follows that although the northern model shows stronger ground motion, the most severe damage in structures should occur in the southern section, because here it is more likely that standard structures, with fundamental periods in the high frequency range, will be strongly excited. The simulations also show that the effect of the rupture reaching the surface cannot be disregarded in predictions of the ground motion in the vicinity of the surface trace. The results presented in this paper provide additional evidence to the assertion that the influence of dynamic source effects on strong ground motion has fundamental importance in the assessment of seismic hazard.

ACKNOWLEDGEMENTS

The cooperation of the Seismology Center, Central Weather Bureau (CWB), Taipei, Taiwan, in making the Chi-Chi

earthquake data available to the authors is kindly acknowledged. The authors received partial support from Conselho Nacional de Pesquisa e Desenvolvimento Tecnológico (CNPq) and from CAPES, Brasil.

REFERENCES

[1] Abrahamson, N.A and Somerville, P.G., "Effects of the hanging wall and footwall on ground motion recorded during the Northridge earthquake", *Bull. Seismol. Soc. Am.*, vol. 86, 1996, pp. 593-599.
[2] Mikumo, T. and Miyatake, T., "Dynamic rupture processes on dipping fault, and estimates of stress drop and strength excess from the results of waveform inversion", *Geophys. J. Int.*, vol. 112, 1993, pp. 481-496.
[3] Shi, B., A., Anooshehpoor, A., Brune, J.N., Zeng, Y., "Dynamics thrust faulting: 2D lattice model", *Bull. Seismol. Soc. Am.*, vol. 88, 1998, pp. 1484-1494.
[4] Oglesby, D.D., Archuleta, R.J. and Nielsen, S.B., "Earthquakes on dipping faults: The effects of broken Symmetry", *Science*, vol. 280, 1998, pp. 1055-1059.
[5] Brune J.N., "Particle motion in a physical model of shallow angle thrust faulting", *Proc. Indian. Cad. Sci.*,vol. 105, 1996, pp. 197-206.
[6] Dalguer, L.A., Irikura, K., Riera J.D. and Chiu, H.C. "Fault Dynamic Rupture Simulation of the hypocenter area of the Thrust Fault of the 1999 Chi-Chi (Taiwan) Earthquake". *In submission to Geophys. Res. Letters*, 2001.
[7] Dalguer, L.A., Irikura, K., Riera J.D. and Chiu, H.C. "The Importance of the Dynamic Source Effects on Strong Ground Motion During the 1999 Chi-Chi (Taiwan) Earthquake: Brief Interpretation of the Damage Distribution on Buildings", *In submission to Bulletin of the Seismological Society of America*, 2001.
[8] Shin T. C., Kuo, K.W., Lee, W.H.K, Teng, T.L. and Tsai, Y.B, "A preliminary report of the 1999 Chi-Chi (Taiwan) earthquake", *Seism. Res. Lett.*,vol. 71, 2000, pp. 24-30.
[9] Nayfeh, A.H. and Hefsy, M.S., "Continuum modeling of three-dimensional truss-like space structures", *AIAA Journal*, vol.,16, 1978, pp. 779-787.
[10] Riera, J.D. and Rocha, M., "A note on the velocity of crack propagation in tensile fracture", *Revista Brasileira de Ciencias Mecanicas, RBCM*, XII, N3, 1991, pp. 217-240.
[11] Doz G.N and Riera J.D., "Towards the numerical simulation of seismic excitation transaction", *13th International Conference on Structural Mechanics in Reactor Technology (SMiRT13)*, vol. 3, Porto Alegre, Brazil, 1995.
[12] Dalguer. L.A., Riera J.D and Irikura, K., 1999, "Simulation of seismic excitation using a stick-slip source mechanism", *Transaction, 15th International Conference on Structural Mechanics in Reactor Technology (SMiRT15)*, vol. 7, pp. 13-18 Seoul, Korea, 1999.